

Variational Mass Perturbation Theory for Light-Front Bound-State Equations

Koji Harada*

Department of Physics, Kyushu University, Fukuoka 812-81, Japan

Thomas Heinzl[†], Christian Stern[‡]

*Institut für Theoretische Physik, Universität Regensburg, Universitätsstraße 31, 93040
Regensburg, Germany*

Abstract

We investigate the mesonic light-front bound-state equations of the 't Hooft and Schwinger model in the two-particle, *i.e.* valence sector, for small fermion mass. We perform a high precision determination of the mass and light-cone wave function of the lowest lying meson by combining fermion mass perturbation theory with a variational approach. All calculations are done entirely in the fermionic representation without using any bosonization scheme. In a step-by-step procedure we enlarge the space of variational parameters. We achieve good convergence so that the calculation of the meson mass squared can be extended to third order in the fermion mass. Within a numerical treatment we include higher Fock states up to six particles. Our results are consistent with all previous numerical investigations, in particular lattice calculations. For the massive Schwinger model, we find a small discrepancy ($\lesssim 2\%$) in comparison with known results. Possible resolutions of this discrepancy are discussed.

PACS number(s): 11.10.Ef, 11.10.St, 11.30.Rd

Typeset using REVTeX

*e-mail: koji@higgs.phys.kyushu-u.ac.jp

†e-mail: thomas.heinzl@physik.uni-regensburg.de

‡e-mail: christian.stern@physik.uni-regensburg.de

I. INTRODUCTION

The number of papers on the Schwinger [1] and 't Hooft [2] [3] models is legion – for a twofold reason. On the one hand, the two models are particularly simple and become, for special choices of parameters, even exactly solvable. On the other hand, despite their simplicity, both models contain interesting physics analogous or similar to properties of gauge theories in higher dimensions. The models therefore serve as interesting theoretical laboratories for studying phenomena like confinement and chiral symmetry breaking, to mention only the most prominent ones. For recent reviews on the two models we refer the reader to [4] for the Schwinger model and to [5] for the 't Hooft model and generalizations thereof.

While confinement (or charge screening) is realized in the same way in both models, via a linearly rising Coulomb potential, the second feature, chiral symmetry breaking, is not. In the 't Hooft model, 1+1 dimensional QCD in the limit of large N_C , chiral symmetry is ‘almost’ spontaneously broken [6] [7] and a *massless* bound state arises in the chiral limit of vanishing quark mass [2] [3]. In the massive Schwinger model, QED in $d = 1+1$ [8] [9], chiral symmetry is anomalously broken, and the contribution of the anomaly to the mass gap survives the chiral limit yielding the free, *massive* boson of the massless model. This boson becomes interacting in the massive model and again can be viewed as a bound state of fermionic constituents. For the sake of brevity we will call the lowest bound state of both models the ‘pion’ (although, in the real world of $d = 3+1$, the Schwinger model boson corresponds to the η' -meson). In this paper we will try to determine its mass and (light-cone) wave function as accurately as possible. We mention in passing that the Schwinger model chiral anomaly is closely related to the appearance of a vacuum θ -angle parameter [10] [11] which also affects the particle spectrum [9]. Throughout this paper, however, we implicitly assume that θ is set to zero.

The calculation of bound state masses and wave functions for the two models at hand has a long history, beginning with the exact solution of the massless Schwinger model [1]. For non-vanishing ‘electron’ mass, m , the model is no longer exactly solvable and one has to resort to approximations. One of them is to assume the mass m being small and expand around the massless solution [8] [9]. For the ‘pion’ mass squared one expects an expansion of the form

$$M^2(m) = 1 + M_1 m + M_2 m^2 + M_3 m^3 + O(m^4) , \quad (1.1)$$

where all masses are measured in units of the basic scale $\mu_0 = e/\sqrt{\pi}$, the mass of the boson in the massless Schwinger model, which is thus represented by the ‘1’ in (1.1). The first order coefficient M_1 was obtained analytically in [12] via bosonization,

$$M_1 = 2e^\gamma = 3.56215 . \quad (1.2)$$

with $\gamma = 0.577216$ being Euler’s constant. Shortly afterwards Bergknoff, using light-cone Hamiltonian techniques (see below), found a value [13]

$$M_1 = 2\pi/\sqrt{3} = 3.62760 , \quad (1.3)$$

which differs from (1.2) by 1.8 %. One topic of the present work will be the analysis of this discrepancy and an attempt to do better by refining 't Hooft's and Bergknoff's methods. This is particularly important as the coefficient M_1 is directly related to the vacuum structure of the Schwinger model by [14]

$$M_1 = -4\pi \langle 0 | \bar{\psi} \psi | 0 \rangle \cos \theta , \quad (1.4)$$

where $\langle 0 | \bar{\psi} \psi | 0 \rangle$ is the condensate of the massless Schwinger model [15] [16] (in units of μ_0),

$$\langle 0 | \bar{\psi} \psi | 0 \rangle = -\frac{1}{2\pi} e^\gamma = -0.28347 , \quad (1.5)$$

and θ the vacuum θ -angle. The result (1.2) thus corresponds to $\theta = 0$. In [17], the relation (1.4) (for $\theta = 0$), which is a 1+1 dimensional analogue of the Gell-Mann-Oakes-Renner formula [18], has been used to determine the condensate from the 'pion' mass squared via

$$\langle 0 | \bar{\psi} \psi | 0 \rangle = -\frac{1}{4\pi} \frac{\partial}{\partial m} M^2(m) \Big|_{m=0} = -\frac{1}{4\pi} M_1 . \quad (1.6)$$

Any inaccuracy in the determination of M_1 thus immediately affects the value of the condensate [19]. At this point it should be mentioned that within light-cone quantization there have been many attempts to calculate the condensate of the massless model alternatively by solving for its vacuum structure [20].

Recently, the calculations of $M^2(m)$ have been extended to second order. Using functional integral techniques and mass perturbation theory, Adam [21] found the analytical expression

$$M_2 = 4\pi^2 \langle 0 | \bar{\psi} \psi | 0 \rangle^2 (A \cos 2\theta + B) , \quad (1.7)$$

where $A = -0.6599$ and $B = 1.7277$ are numerical constants, given in terms of integral expressions containing the 'pion' propagator for $m = 0$. Inserting the values for A , B and the condensate, and setting $\theta = 0$, (1.7) becomes

$$M_2 = 3.3874 . \quad (1.8)$$

This result has been confirmed independently by Fields et al. [22], who derived the same integral expressions by summing up all relevant Feynman diagrams in the bosonized theory using near-light-cone coordinates.

To first order in m , the mass-squared of the 't Hooft model 'pion' has already been calculated by 't Hooft [3] by solving the associated light-front bound-state equation. He derived this equation by projecting the covariant Bethe-Salpeter equation onto three-dimensional hypersurfaces of equal light-cone time, x^+ . Soon afterwards, the equation was rederived using light-cone Hamiltonian techniques [23]. The result for the 'pion' mass-squared is

$$M^2(m) = 2 \frac{\pi}{\sqrt{3}} m + O(m^2) . \quad (1.9)$$

As the light-front bound state equations of the two models at hand differ only by an additive contribution due to the anomaly (see [17] [24] and below), it is not too surprising that

't Hooft's and Bergknoff's results coincide. For the 't Hooft model, all masses are expressed in units of the basic scale $\mu_0^2 = g^2 N_C / 2\pi$ ¹. It is obvious from (1.9) that M^2 vanishes in the chiral limit, $m \rightarrow 0$. As explained in [6] [7], this is not in contradiction with Coleman's theorem [25] as the 'pion' is not a Goldstone boson and decouples from the S -matrix.

The condensate of the 't Hooft model has first been calculated by Zhitnitsky using sum rule techniques [7],

$$\langle 0 | \bar{\psi} \psi | 0 \rangle / N_C = -\frac{1}{4\pi} M_1 = -0.28868 . \quad (1.10)$$

As expected, the condensate is proportional to N_C and can again be written in terms of M_1 . The result has been confirmed analytically [26] [27] and numerically [28]. Via (1.10), the numerical value [28] for the condensate leads to a numerical estimate for M_1 ,

$$M_1 = 3.64 \pm 0.05 . \quad (1.11)$$

Though the numerical calculation did not use light-front methods, it seems to favour the 't Hooft-Bergknoff value (1.3), which is *the* standard value for the 't Hooft model. Higher order corrections to (1.9) have been discussed in [29] without explicit calculation of the expansion coefficients.

In recent years, both models have been serving as a testing ground for new techniques developed in order to solve bound state problems using light-cone (or, equivalently, light-front) quantization. These new methods are 'discretized light-cone quantization' (DLCQ) [30] [31], where one works in a finite volume leading to an equally-spaced momentum grid, and the 'light-front Tamm-Dancoff (LFTD) approximation' [32], which (drastically) truncates the Fock space of the continuum theory thus limiting the number of constituents a bound state can have. The latter approach can be viewed as a generalization of the techniques of 't Hooft and Bergknoff. Both methods aim at a numerical solution of relativistic bound state problems. DLCQ has been applied to the massive Schwinger model [33] and to QCD in 1+1 dimensions (for arbitrary N_C) [24] [34]. There are analogous LFTD calculations for both models, QCD₁₊₁ [35] [36] and the Schwinger model [37] [38]. These latter works are closer in spirit to ours than the DLCQ approaches. We will compare to all this recent work in more detail later on.

The purpose of this paper is to obtain the 'pion' mass squared of both the Schwinger and 't Hooft model to high accuracy including the third order in m . In addition, we want to calculate the light-cone wave function of the 'pion' with high precision. We will use the light-front techniques of 't Hooft and Bergknoff and extensions thereof. Our starting point is a LFTD truncation to the two-particle sector. The low order calculations will be done analytically. To go beyond, computer algebraic and numerical methods will be applied and their convergence tested. The final goal is to shed some light on the advantages and limitations of this particular light front approach to bound-state equations.

¹Some authors (including 't Hooft) use a different convention for the coupling, which amounts to the replacement $g^2 \rightarrow 2g^2$.

The paper is organized as follows. In Section II we review 't Hooft's ansatz for the wave function yielding the lowest order solution of the bound-state equation. We compare the exact endpoint analysis with a variational procedure which is introduced at this point. In Section III we extend 't Hooft's ansatz by adding more variational parameters in such a way that an analytic solution can still be obtained. To this end we employ computer algebraic methods which allow to treat up to five variational parameters. This is sufficient to achieve rather good convergence. In Section IV, these results are compared with the outcome of purely numerical calculations. We conclude the paper in Section V with some discussion of the presented as well as related work.

II. 'T HOOFT'S ANSATZ

Our starting point is the bound state equation of the 't Hooft and Schwinger model in the two-particle sector, which, in a unified way, can be written as [17] [24]

$$M^2\phi(x) = (m^2 - 1)\frac{\phi(x)}{x(1-x)} - \mathcal{P} \int_0^1 dy \frac{\phi(y)}{(x-y)^2} + \alpha \int_0^1 dx \phi(x) . \quad (2.1)$$

We will refer to this equation as the 't Hooft-Bergknoff equation in what follows. $\phi(x)$ denotes the valence part of the 'pion' wave function, x and y the momentum fraction of one of the two fermions in the meson. The symbol \mathcal{P} indicates that the integral is defined as a principal value [2] [39].

The parameter α measures the strength of the anomaly. In the 't Hooft model, $\alpha = 0$ (no anomaly), and in the Schwinger model $\alpha = 1$ (representing the usual chiral anomaly). The scale parameters, as already mentioned, are given by $\mu_0^2 = g^2 N_C / 2\pi$ and $\mu_0^2 = e^2 / \pi$, respectively. M denotes the mass of the lowest lying bound state (the 'pion'). Our objective is to obtain (approximate, but accurate) solutions for M and ϕ .

Upon multiplying (2.1) with $\phi(x)$ and integrating over x we obtain for the eigenvalue

$$M^2(m) = (m^2 - 1)\frac{I_1}{I_0} - \frac{I_2}{I_0} + \alpha\frac{I_3^2}{I_0} , \quad (2.2)$$

where we have defined the integrals

$$I_0 = \int_0^1 dx \phi^2(x) , \quad (2.3)$$

$$I_1 = \int_0^1 dx \frac{\phi^2(x)}{x(1-x)} , \quad (2.4)$$

$$I_2 = \mathcal{P} \int_0^1 dx dy \frac{\phi(x)\phi(y)}{(x-y)^2} , \quad (2.5)$$

$$I_3 = \int_0^1 dx \phi(x) . \quad (2.6)$$

I_0 is the norm of the wave function, I_1 and I_2 are matrix elements of the mass and interaction term in the light-cone Hamiltonian [13] [37] in the state $|\phi\rangle$. The integral I_3 is the wave

function at the origin. An independent formula for the ‘pion’ mass-squared is obtained by integrating (2.1) over x . This results in the simple expression

$$M^2(m) = m^2 \frac{I_4}{I_3} + \alpha, \quad (2.7)$$

with the additional integral,

$$I_4 = \int_0^1 dx \frac{\phi(x)}{x(1-x)}. \quad (2.8)$$

Of course, for the exact wave functions, the right-hand sides of (2.2) and (2.7) have to coincide. As the wave functions cannot be obtained exactly, we will later use the agreement between both values for the mass-squared as a measure for the accuracy of our wave functions. To determine the latter we will use a particular class of variational ansätze.

In his original work on the subject, [2] [3], ’t Hooft used the following ansatz for the wave function

$$\phi(x) = x^\beta(1-x)^\beta. \quad (2.9)$$

This ansatz is symmetric in $x \leftrightarrow 1-x$ (charge conjugation odd), and β is supposed to lie between zero and one so that the endpoint behaviour is non-analytic. As a non-trivial boundary condition one has the exact solution of the massless case,

$$M^2 = \alpha, \quad \text{and} \quad \phi(x) = 1, \quad \text{i.e.} \quad \beta = 0. \quad (2.10)$$

The main effect of having a non-vanishing fermion mass is the vanishing of the wave functions at the endpoints implying a non-zero β . This suggests the following series expansion for β ,

$$\beta(m) = \beta_1 m + \beta_2 m^2 + \beta_3 m^3 + O(m^4), \quad (2.11)$$

and for the ‘pion’ mass squared,

$$M^2 = \alpha + M_1 m + M_2 m^2 + M_3 m^3 + O(m^4), \quad (2.12)$$

in accordance with (1.1).

A. Exact Endpoint Behaviour

The exponent β in (2.9) can actually be determined exactly by studying the small- x behaviour of the bound state equation (2.1). To this end we evaluate the principal value integral for $x \rightarrow 0$,

$$\begin{aligned} \mathcal{P} \int_0^1 dy \frac{y^\beta(1-y)^\beta}{(x-y)^2} &= x^{\beta-1} \left[\mathcal{P} \int_0^\infty dz \frac{z^\beta}{(1-z)^2} + O(x) \right] \\ &= -x^{\beta-1} \left[\pi\beta \cot \pi\beta + O(x) \right]. \end{aligned} \quad (2.13)$$

Plugging this into (2.1) and demanding the coefficient of $x^{\beta-1}$ to vanish yields the transcendental equation [2]

$$m^2 - 1 + \pi\beta \cot \pi\beta = 0, \quad (2.14)$$

which is independent of the anomaly α . Using this expression we can determine β either numerically for arbitrary m or analytically for small m by expanding

$$\beta = \frac{\sqrt{3}}{\pi} m \left(1 - \frac{1}{10} m^2 \right) + O(m^4). \quad (2.15)$$

Note that the second order coefficient, β_2 , is vanishing. Furthermore, for the exact β one has $\beta_1/\beta_3 = -1/10$, which we will use as a check for our numerical results later on.

Our task is now to determine the coefficients M_i , $i = 1, 2, 3$ in (2.12). The ansatz (2.9) leads to the following results for the for the ‘pion’ mass squared (2.2),

$$\begin{aligned} M^2(m, \beta) &= (m^2 - 1) \left(\frac{1}{\beta} + 4 \right) \\ &+ \left(\frac{1}{4} + \beta \right) \frac{B^2(\beta, \beta)}{B(2\beta, 2\beta)} \left[1 + \alpha \frac{\beta}{(2\beta + 1)^2} \right]. \end{aligned} \quad (2.16)$$

In the above, $B(z_1, z_2)$ denotes the Beta function. The relevant formulae for double integrals like I_2 (2.5) can be found in [40] and [41], Appendix C. For $\alpha = 0$, (2.16) has also been obtained in [36]. Let us emphasize that this result, which expresses the ‘pion’ mass squared as a function of the (exactly known) endpoint exponent β , is only approximate as ‘t Hooft’s ansatz (2.9) for the wave function does *not* represent an exact solution of the bound-state equation. It is only the endpoint behaviour that is known exactly; in the intermediate- x region ‘t Hooft’s ansatz is only an approximation that presumably becomes rather bad for large masses (non-relativistic limit) where the wave function is strongly peaked at $x = 1/2$. The accuracy of the result will be discussed extensively later on.

In order to find M^2 to order m^3 we need to expand (2.16) to order β^3 , as β itself is of order m . The result is

$$\begin{aligned} M^2(m, \beta) &= \frac{m^2}{\beta} + 4m^2 + \alpha + \frac{\pi^2}{3}\beta \\ &+ 4 \left[\pi^2/3 - 3\zeta(3) + \alpha(\pi^2/12 - 1) \right] \beta^2 \\ &+ \left[\frac{3}{5}\pi^4 - 48\zeta(3) + 4\alpha(4 - 3\zeta(3)) \right] \beta^3 \\ &+ O(\beta^4). \end{aligned} \quad (2.17)$$

Inserting β from (2.15) one finds

$$\begin{aligned} M^2(m) &= \alpha + 2 \frac{\pi}{\sqrt{3}} m \\ &+ \left[4 \left(2 - \frac{9}{\pi^2} \zeta(3) \right) + \alpha \left(1 - \frac{12}{\pi^2} \right) \right] m^2 \end{aligned}$$

$$\begin{aligned}
& + \frac{3\sqrt{3}}{\pi^3} \left[\left(\frac{3}{5}\pi^4 - 48\zeta(3) \right) + 4\alpha(4 - 3\zeta(3)) \right] m^3 \\
& + O(m^4) .
\end{aligned} \tag{2.18}$$

Let us give the explicit results for the 't Hooft and Schwinger model, *i.e.* for $\alpha = 0$ and $\alpha = 1$, respectively. For $\alpha = 0$, we have

$$M_1 = 2\frac{\pi}{\sqrt{3}} = 3.627599 , \tag{2.19}$$

$$M_2 = 4\left(2 - \zeta(3)\frac{9}{\pi^2}\right) = 3.615422 , \tag{2.20}$$

$$M_3 = \frac{3\sqrt{3}}{\pi^3} \left(\frac{3}{5}\pi^4 - 48\zeta(3) \right) = 0.125139 , \tag{2.21}$$

and for $\alpha = 1$,

$$M_1 = 2\frac{\pi}{\sqrt{3}} = 3.627599 , \tag{2.22}$$

$$M_2 = 4\left(2 - \zeta(3)\frac{9}{\pi^2}\right) + 1 - \frac{12}{\pi^2} = 3.399568 , \tag{2.23}$$

$$\begin{aligned}
M_3 & = \frac{3\sqrt{3}}{\pi^3} \left[\left(\frac{3}{5}\pi^4 - 48\zeta(3) \right) + 4(4 - 3\zeta(3)) \right] \\
& = 0.389137 .
\end{aligned} \tag{2.24}$$

We note that the anomaly does *not* contribute to the first order term which therefore is the same in both the Schwinger and 't Hooft model. This confirms the observation made in the introduction, the coincidence of (1.3) and (1.9). As M_1 is proportional to the condensate, *cf.* (1.6) and (1.10), the latter is also independent of the anomaly [17].

For the Schwinger model ($\alpha = 1$), the second order result can be compared with the analytical calculation of Adam, (1.8). Astonishingly, the relative difference is smaller than for the first order, namely 0.36 %. This is accidental, as we shall see below.

As a cross check, we determine the 'pion' mass squared using the alternative formula (2.7). Plugging in the ansatz (2.9), we find the fairly simple expression

$$\tilde{M}^2(m, \beta) = 4m^2 + \alpha + \frac{2m^2}{\beta} . \tag{2.25}$$

Inserting the expansion (2.15) this becomes

$$\tilde{M}^2 = \alpha + \tilde{M}_1 m + \tilde{M}_2 m^2 + \tilde{M}_3 m^3 + O(m^4) , \tag{2.26}$$

with the coefficients \tilde{M}_i explicitly given by

$$\tilde{M}_1 = 2\pi/\sqrt{3} = 3.627599 , \tag{2.27}$$

$$\tilde{M}_2 = 4 , \tag{2.28}$$

$$\tilde{M}_3 = \tilde{M}_1/10 = 0.3627599 . \tag{2.29}$$

In (2.26) the anomaly contributes only in zeroth order (as β is independent of α), so that the \tilde{M}_i are the same for $\alpha = 0$ and $\alpha = 1$. Comparing with (2.19) and (2.22), we see that the first order coefficients coincide for the two alternative mass formulae. In addition, one finds that \tilde{M}_2 roughly coincides with the M_2 of both the 't Hooft and Schwinger model to within 10-20 %. The value for \tilde{M}_3 is smaller by approximately an order of magnitude.

We conclude that 't Hooft's ansatz works well to lowest non-trivial order in m but needs improvement if one wants to go further. As a preparative step for such a development we now introduce a variational method that can easily be extended to accurately calculate higher orders in m .

B. Variational Approach

At variance with the above we are now going to regard β as a variational parameter to be determined by minimizing the function $M^2(m, \beta)$ of (2.17). To this end we insert the expansion (2.11) into (2.17) and obtain

$$\begin{aligned}
M^2(m) &= \alpha + \left(\frac{\pi^2}{3} \beta_1 + \frac{1}{\beta_1} \right) m \\
&+ \left[4 + \beta_2 \left(\frac{\pi^2}{3} - \frac{1}{\beta_1^2} \right) \right. \\
&+ \left. 4 \left(\frac{\pi^2}{3} - 3\zeta(3) + \alpha \left(\frac{\pi^2}{12} - 1 \right) \right) \beta_1^2 \right] m^2 \\
&+ \left[8\beta_1\beta_2 \left(\frac{\pi^2}{3} - 3\zeta(3) \right) + \beta_1^3 \left(\frac{3}{5}\pi^4 - 48\zeta(3) \right) \right. \\
&+ \left. \frac{\beta_2^2}{\beta_1^3} + \beta_3 \left(\frac{\pi^2}{3} - \frac{1}{\beta_1^2} \right) \right. \\
&+ \left. \alpha \left(2\beta_1\beta_2 \left(\frac{\pi^2}{3} - 4 \right) + 4\beta_1^3 (4 - 3\zeta(3)) \right) \right] m^3 \\
&+ O(m^4) .
\end{aligned} \tag{2.30}$$

Note that to order m only the leading coefficient β_1 contributes. We will furthermore shortly see that the dependence of M_2 on β_2 and of M_3 on β_3 is only apparent.

Solving the minimization equation, $\partial M^2 / \partial \beta = 0$, for the coefficients β_i , leads to

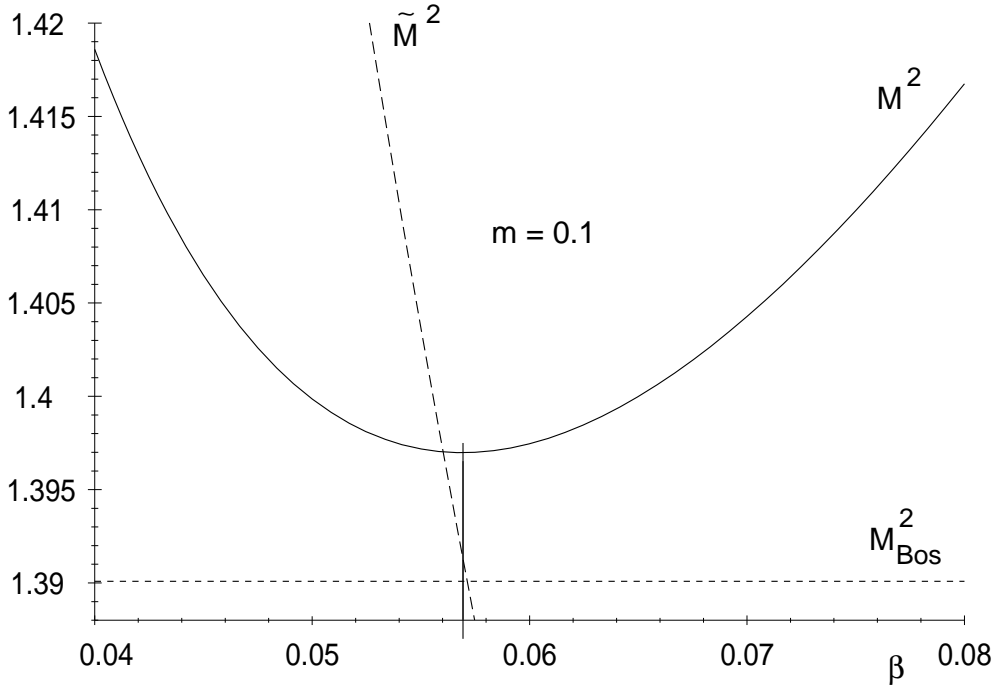
$$\beta_1 = \sqrt{3}/\pi = 0.55133 , \tag{2.31}$$

$$\beta_2 = 0.11690 + 0.065612\alpha , \tag{2.32}$$

$$\beta_3 = 0.0049077 - 0.050811\alpha + 0.019521\alpha^2 . \tag{2.33}$$

Comparing with (2.15) we note that the coefficient β_1 is exact! Plugging it into (2.30) we verify the statement above that M_2 is independent of β_2 and M_3 independent of β_3 . Therefore, the expressions (2.30) and (2.18) coincide up to and including order m^2 . M_1 and M_2 are thus the same, irrespective of whether one uses the exact endpoint exponent of (2.15) or its variational estimate. The estimates (2.31-2.33) for the coefficients β_i differ in at

FIG. 1. Comparison of the two alternative mass formulae, (2.16) for $M^2(\beta)$ and (2.25) for $\tilde{M}^2(\beta)$, and the second order bosonization results [21] [22] for $m = 0.1$. The vertical line marks the minimum of the curve $M^2(\beta)$ yielding the variational estimate for β using 't Hooft's ansatz. For this value of β one finds $M^2(m = 0.1) = 1.3969$ and $\tilde{M}^2(m = 0.1) = 1.3913$. The bosonization result (short-dashed horizontal line) is $M_{\text{Bos}}^2(m = 0.1) = 1.390 \pm 1 \cdot 10^{-3}$, where the error is basically an estimate of the unknown third order coefficient. Thus, within 't Hooft's ansatz, the alternative mass formula yields a somewhat better result at $m = 0.1$. In the next sections we will refine our methods so that the variational estimates for M^2 and \tilde{M}^2 will converge towards each other.



least three respects from the exact values of (2.15): (i) β_2 and β_3 depend on α , (ii) $\beta_2 \neq 0$, (iii) $\beta_3 \neq -\beta_1/10$. However, all these shortcomings affect at most the third order coefficient M_3 , and thus become negligible for small m . Only if one wants to have reliable numbers for M_3 , (which we will be going to produce), these effects have to be taken into account. The present values of β_i lead to

$$\begin{aligned} M_3(\alpha = 0) &= 0.043597, \\ M_3(\alpha = 1) &= 0.190372, \end{aligned} \tag{2.34}$$

which should be compared with (2.21) and (2.24), respectively. The differences are large so that the agreement is not particularly good. These discrepancies, however, are not disturbing at this point, as we are calculating a third order effect with just one variational parameter. We will do better later on by enlarging the number of these parameters until we see satisfactory convergence of the results.

The variational estimate for β can also be plugged into the alternative mass formula, $\tilde{M}^2(m, \beta)$, (2.25), which by itself does not constitute a variational problem. We do not give

the analytical results for the \tilde{M}_i here but simply refer to Fig. 1 for a qualitative comparison of the two alternative formulae, and to Section III, Tables III and VI, for the actual numbers.

As stated repeatedly, 't Hooft's ansatz (2.9) used so far has to be extended if one wants to accurately determine the second and third order coefficients of M^2 . This is our next issue.

III. EXTENSION OF 'T HOOFT'S ANSATZ

For the numerical calculations of [36] [38] [41] the following set of trial functions has been used:

$$\phi(x) = \sum_{k=0}^N u_k [x(1-x)]^{\beta+k} . \quad (3.1)$$

Obviously, the term with $k = 0$ and normalization $u_0 = 1$ corresponds to 't Hooft's original ansatz (2.9). The coefficients u_k are treated as additional variational parameters, so that, according to the variational principle, (3.1) *must* yield a better result than (2.9). The question is, how big the improvement will be. To this end we will calculate the coefficients M_i by adding more and more basis functions to 't Hooft's original ansatz (2.9), thus enlarging our space of variational parameters. We will follow the two different approaches mentioned above, namely, (i) use the exact β from (2.15), or, (ii) treat β as one of the variational parameters. For both approaches we will compare the calculated coefficients M_i with the \tilde{M}_i obtained from the alternative mass formula (2.7). We will continue adding basis functions until we see our results converge. The maximum number N of basis functions in this section will be five, *i.e.* 't Hooft's original wave function plus four corrections.

A particular benefit of the ansatz (3.1) is the fact that the integrals I_1 to I_4 can still be evaluated analytically though the formulae become rather lengthy. For this reason we will make heavy use of the program package MAPLE in what follows. As a result we have analytical expressions for all the quantities we calculate. As these expressions cover pages and pages without being very instructive, we do not display them but rather the evaluated numbers. In this sense, our treatment might be called 'semi-analytical'. A major advantage, however, of using computer algebraic manipulations is the high calculational accuracy which is only limited by the maximum number of digits the machine can handle.

A. Purely Variational Approach

In this subsection, β will always be treated as a variational parameter and thus be obtained by minimizing the 'pion' mass squared, M^2 . In the ansatz (3.1) we use up to four additional basis functions, so that our maximum N is four. To avoid an inflation of indices we rename the coefficients u_k , $k = 1, \dots, 4$ by a , b , c and d , respectively. Their expansion coefficients, defined via

$$\begin{aligned} a &= a_1 m + a_2 m^2 , \\ b &= b_1 m + b_2 m^2 , \\ c &= c_1 m + c_2 m^2 , \\ d &= d_1 m + d_2 m^2 , \end{aligned} \quad (3.2)$$

are determined (recursively) by minimizing M^2 with respect to them. Let us start with the 't Hooft model ($\alpha = 0$).

1. 't Hooft Model

In order to save space we do not display all the values for the coefficients in (3.2). The best values obtained are given in the last section when we discuss the quality of the wave function. Here, we rather display the results for the coefficients β_i of β (see Table I), as these can be compared with the exact values of (2.15).

As an important finding we note that β_1 remains unchanged at the exact value $\sqrt{3}/\pi$ (a 'variational invariant'). β_2 tends to zero, as it should. The non-vanishing of β_2 only affects the coefficient M_3 , as M_1 and M_2 do not depend on β_2 . The convergence of β_3 towards $-\beta_1/10$ seems somewhat slow; but as all M_i , $i = 1, 2, 3$, are independent of β_3 this has no observable effect.

In Table II we list the expansion coefficients of the mass squared, M^2 . One notes that the convergence of the results for M_2 and M_3 is rather good. For M_2 we finally have a relative accuracy of $8 \cdot 10^{-7}$, and for M_3 of $4 \cdot 10^{-5}$. Furthermore, the coefficients are getting smaller if one adds more basis functions, in accordance with the variational principle. As the coefficient M_1 is entirely determined by the 'variational invariant' β_1 it remains unchanged at $2\pi/\sqrt{3}$. This is another important result: M_1 stays fixed at the standard 't Hooft-Bergknoff value (1.3).

If we use the alternative mass formula (2.7) and evaluate it using the wave function calculated above we find the values for \tilde{M}^2 listed in Table III.

It should be pointed out that the values of the \tilde{M}_i are somewhat more sensitive to the values of the expansion coefficients β_i , because \tilde{M}_2 does depend on β_2 , and \tilde{M}_3 on β_2 and β_3 . To check the quality of our wave functions one should compare the results for M_i and \tilde{M}_i which are listed in Tables II and III. Once more it is gratifying to note that we are improving our results step by step in the variational procedure. The values of \tilde{M}_i converge towards those of M_i . The relative accuracy is approximately 10^{-3} . This error is entirely due to the difference between the calculated and the real wave function. It is clear that the accuracy in the single eigenvalue M^2 (Table II) is higher than the one for the wave function, where in principle an infinite number of points have to be calculated. This represents an indirect proof that we are indeed improving our wave functions, and not just the eigenvalues.

2. Schwinger Model

For the Schwinger model ($\alpha = 1$), we perform exactly the same calculations. The expansion coefficients of β are listed in Table IV. Although the coefficients β_2 , β_3 are somewhat different from those in Table I (which they must be as they lose their dependence on α only in the strict limit of *exact* evaluation) we note the same tendency: β_2 converges to zero and β_3 towards $-\beta_1/10$.

The best values for the 'pion' mass squared are again provided by the variational results listed in Table V. The numerical accuracy is practically the same as for the analogous Ta-

TABLE I. Expansion coefficients of the end point exponent β for the 't Hooft model obtained by successively varying with respect to β (first line) , β and a (second line), etc. The first column, β_1 , coincides with the result from the exact endpoint analysis, which in addition yields $\beta_2 = 0$, $\beta_3 = -\beta_1/10$.

| <i>Ansatz</i> | $\beta_1 = \sqrt{3}/\pi$ | β_2 | β_3 |
|---------------|--------------------------|------------|-------------|
| 't Hooft | 0.55132889 | 0.11689763 | 0.00490773 |
| a | 0.55132889 | 0.00976951 | -0.04010634 |
| b | 0.55132889 | 0.00256081 | -0.04889172 |
| c | 0.55132889 | 0.00102086 | -0.05209341 |
| d | 0.55132889 | 0.00050738 | -0.05343097 |

TABLE II. Expansion coefficients of M^2 for the 't Hooft model obtained by successively enlarging the space of variational parameters. M_1 is the standard 't Hooft-Bergknoff result. Note the good convergence towards the bottom of the table.

| <i>Ansatz</i> | $M_1 = 2\pi/\sqrt{3}$ | M_2 | M_3 |
|---------------|-----------------------|------------|-------------|
| 't Hooft | 3.62759873 | 3.61542218 | 0.043597197 |
| a | 3.62759873 | 3.58136872 | 0.061736701 |
| b | 3.62759873 | 3.58107780 | 0.061805257 |
| c | 3.62759873 | 3.58105821 | 0.061795547 |
| d | 3.62759873 | 3.58105532 | 0.061793082 |

TABLE III. Expansion coefficients of the alternative mass squared \tilde{M}^2 for the 't Hooft model obtained by successively enlarging the space of variational parameters. Again, the fixed value for \tilde{M}_1 is the standard 't Hooft-Bergknoff result.

| <i>Ansatz</i> | $\tilde{M}_1 = 2\pi/\sqrt{3}$ | \tilde{M}_2 | \tilde{M}_3 |
|---------------|-------------------------------|---------------|---------------|
| 't Hooft | 3.62759873 | 3.23084437 | 0.130791594 |
| a | 3.62759873 | 3.54922830 | 0.066592425 |
| b | 3.62759873 | 3.57265307 | 0.059652468 |
| c | 3.62759873 | 3.57769969 | 0.060282959 |
| d | 3.62759873 | 3.57938609 | 0.060854772 |

TABLE IV. Expansion coefficients of the endpoint exponent β for the Schwinger model obtained by successively enlarging the space of variational parameters. The first column, β_1 , coincides with the result from the exact endpoint analysis, which in addition yields $\beta_2 = 0$, $\beta_3 = -\beta_1/10$.

| <i>Ansatz</i> | β_1 | β_2 | β_3 |
|---------------|------------|------------|--------------|
| 't Hooft | 0.55132889 | 0.18250945 | -0.026382222 |
| a | 0.55132889 | 0.01177681 | -0.040372413 |
| b | 0.55132889 | 0.00317437 | -0.048081756 |
| c | 0.55132889 | 0.00127507 | -0.051602713 |
| d | 0.55132889 | 0.00063609 | -0.053130398 |

TABLE V. Expansion coefficients of M^2 for the Schwinger model obtained by successively enlarging the space of variational parameters. Again, the fixed value for M_1 is the standard 't Hooft-Bergknoff result. Note the good convergence towards the bottom of the table.

| <i>Ansatz</i> | $M_1 = 2\pi/\sqrt{3}$ | M_2 | M_3 |
|---------------|-----------------------|------------|------------|
| 't Hooft | 3.62759873 | 3.39956798 | 0.19037224 |
| a | 3.62759873 | 3.30906326 | 0.34776772 |
| b | 3.62759873 | 3.30864244 | 0.34820193 |
| c | 3.62759873 | 3.30861240 | 0.34820513 |
| d | 3.62759873 | 3.30860791 | 0.34820389 |

TABLE VI. Expansion coefficients of the alternative mass squared \tilde{M}^2 for the Schwinger model obtained by successively enlarging the space of variational parameters. Again, the fixed value for \tilde{M}_1 is the standard 't Hooft-Bergknoff result.

| <i>Ansatz</i> | $\tilde{M}_1 = 2\pi/\sqrt{3}$ | \tilde{M}_2 | \tilde{M}_3 |
|---------------|-------------------------------|---------------|---------------|
| 't Hooft | 3.62759873 | 2.79913596 | 0.57111672 |
| a | 3.62759873 | 3.27031909 | 0.36868190 |
| b | 3.62759873 | 3.29819920 | 0.34869835 |
| c | 3.62759873 | 3.30441759 | 0.34753576 |
| d | 3.62759873 | 3.30651525 | 0.34762562 |

ble II. The comparison with the alternatively calculated coefficients \tilde{M}^2 is given in Table VI. Again, everything is completely analogous to the case of the 't Hooft model ($\alpha = 0$).

B. Variational Approach using the exact β

In this subsection we calculate M^2 and \tilde{M}^2 for both values of α using the exact value (2.15) for β . Thus only a, b, c, d are treated as variational parameters. This is the procedure employed numerically in [38]. From the discussion of the preceding subsection, in particular the values for the β_i displayed in Table I, which differ minimally from the exact values, we expect that the results will be very close to those from the purely variational approach.

1. 't Hooft Model

This is exactly what happens as can be seen from Tables VII and VIII. Comparing Table VII with Table II one finds that the coefficients M_1 and M_2 of both tables coincide as these only depend on β_1 which is the same in both approaches. Only for M_3 there are slight differences, due to the dependence on β_2 . For the \tilde{M}_i , $i = 2, 3$, the discrepancies are somewhat bigger as these coefficients do depend on β_2 and β_3 (Table III *vs.* Table VIII). Still the consistency is quite obvious.

Upon comparing the second columns of Tables II and III, respectively Tables VII and VIII, one notes a funny coincidence. In the first case M_2 is slightly bigger than \tilde{M}_2 , and vice versa in the second case. If one denotes the purely variational results with a superscript 'v', and the results obtained with the exact β with a superscript 'e', one finds that M_2 , which is the same in both approaches, is given by the arithmetic mean

$$M_2 = \frac{1}{2} \left(\tilde{M}_2^e + \tilde{M}_2^v \right) . \quad (3.3)$$

We have checked this analytically for 't Hooft's ansatz. For the higher orders this is difficult to do but the numerical evidence is beyond doubt.

Comparing the third columns of Tables II and VII, one finds that $M_3^v < M_3^e$. We thus see a slight tendency that the results of the purely variational procedure are better than those obtained using the exact β . The same observation has been made by Mo and Perry [37], in particular for large values of the fermion mass m (where the third order coefficient M_3 becomes important). We interpret this fact as a hint that for larger m the behaviour of the wave function in the intermediate region becomes more relevant compared to the endpoint behaviour.

2. Schwinger Model

For the Schwinger model, the analogous results are listed in Tables IX and X. Exactly the same remarks as above apply including the size of the errors and the relation between M_2 and $\tilde{M}_2^e, \tilde{M}_2^v$. In the next section we will verify our results by purely numerical methods.

TABLE VII. Expansion coefficients of M^2 ('t Hooft model) obtained by using the exact endpoint exponent β and successively enlarging the space of variational parameters.. Again, the fixed value for M_1 is the standard 't Hooft-Bergknoff result.

| <i>Ansatz</i> | $M_1 = 2\pi/\sqrt{3}$ | M_2 | M_3 |
|---------------|-----------------------|------------|------------|
| 't Hooft | 3.62759873 | 3.61542219 | 0.12513878 |
| a | 3.62759873 | 3.58136873 | 0.06230622 |
| b | 3.62759873 | 3.58107781 | 0.06184441 |
| c | 3.62759873 | 3.58105821 | 0.06180178 |
| d | 3.62759873 | 3.58105533 | 0.06179462 |

TABLE VIII. Expansion coefficients of the alternatively defined mass squared \tilde{M}^2 ('t Hooft model) obtained by using the exact endpoint exponent β and successively enlarging the space of variational parameters. Again, the fixed value for \tilde{M}_1 is the standard 't Hooft-Bergknoff result.

| <i>Ansatz</i> | $\tilde{M}_1 = 2\pi/\sqrt{3}$ | \tilde{M}_2 | \tilde{M}_3 |
|---------------|-------------------------------|---------------|---------------|
| 't Hooft | 3.62759873 | 4.0 | 0.36275987 |
| a | 3.62759873 | 3.61350915 | 0.08659575 |
| b | 3.62759873 | 3.58950254 | 0.07106398 |
| c | 3.62759873 | 3.58441672 | 0.06603497 |
| d | 3.62759873 | 3.58272458 | 0.06406179 |

TABLE IX. Expansion coefficients of M^2 (Schwinger model) obtained by using the exact endpoint exponent β and successively enlarging the space of variational parameters. Again, the fixed value for M_1 is the standard 't Hooft-Bergknoff result.

| <i>Ansatz</i> | $M_1 = 2\pi/\sqrt{3}$ | M_2 | M_3 |
|---------------|-----------------------|------------|------------|
| 't Hooft | 3.62759873 | 3.39956798 | 0.38913656 |
| a | 3.62759873 | 3.30906326 | 0.34859533 |
| b | 3.62759873 | 3.30864244 | 0.34826210 |
| c | 3.62759873 | 3.30861239 | 0.34821485 |
| d | 3.62759873 | 3.30860791 | 0.34820630 |

TABLE X. Expansion coefficients of the alternatively defined mass squared \tilde{M}^2 (Schwinger model) obtained by using the exact endpoint exponent β and successively enlarging the space of variational parameters. Again, the fixed value for \tilde{M}_1 is the standard 't Hooft-Bergknoff result.

| <i>Ansatz</i> | $\tilde{M}_1 = 2\pi/\sqrt{3}$ | \tilde{M}_2 | \tilde{M}_3 |
|---------------|-------------------------------|---------------|---------------|
| 't Hooft | 3.627598730 | 4.0 | 0.3627598730 |
| a | 3.627598730 | 3.347807427 | 0.3637551073 |
| b | 3.627598730 | 3.319085690 | 0.3566261465 |
| c | 3.627598730 | 3.312807215 | 0.3523062162 |
| d | 3.627598730 | 3.310700593 | 0.3504584408 |

TABLE XI. Numerical results using lowest order (two-particle) LFTD approximation for $M^2 - 1$ as a function of the fermion mass m , for $\alpha = 1$ (Schwinger model).

| <i>Ansatz</i> | $m = 0.0001$ | $m = 0.0005$ | $m = 0.001$ | $m = 0.005$ | $m = 0.01$ | $m = 0.05$ | $m = 0.1$ | $m=0.3$ | $m=0.5$ |
|---------------|--------------|--------------|-------------|-------------|------------|------------|-----------|----------|----------|
| 't Hooft | 0.000362794 | 0.00181465 | 0.00363100 | 0.0182230 | 0.0366163 | 0.189927 | 0.397130 | 1.403677 | 2.705008 |
| a | 0.000362858 | 0.00181465 | 0.00363086 | 0.0182207 | 0.0366072 | 0.189695 | 0.396181 | 1.394169 | 2.675165 |
| b | – | 0.00181461 | 0.00363100 | 0.0182210 | 0.0366071 | 0.189694 | 0.396176 | 1.394129 | 2.675072 |
| c | – | 0.00181459 | – | – | 0.0366071 | 0.189694 | 0.396176 | 1.394125 | 2.675059 |
| d | – | – | – | – | 0.0366073 | 0.189694 | 0.396176 | 1.394125 | 2.675057 |
| e | – | – | – | – | – | – | – | 1.394123 | 2.675058 |

IV. COMPARISON WITH NUMERICAL RESULTS

For the numerical calculations the ansatz (3.1) has been used. The value for β has been determined numerically from (2.14). Again, up to four additional basis functions have been included (for larger masses even five). Let us begin with the Schwinger model ($\alpha = 1$). Here we can use the code developed in [38]. In Table XI we list $M^2 - 1$ as a function of the fermion mass m , calculated within two-particle LFTD approximation. The notations a,b,c,d are as in the preceding section, the letter ‘e’ denotes the inclusion of a fifth basis function.

One main difference in comparison with the computer algebraic treatment of Section III is the numerical inaccuracy for small m . This is a general disease of numerical treatments, and also shared *e.g.* by the lattice [14], [15] or DLCQ approach [33]. In these approaches, however, the numerical errors are typically much larger than ours (see the next section for an explicit comparison). Due to the small- m instability, our numerical calculation does not converge within an arbitrary number of digits. As soon as a calculated value for $M^2 - 1$ becomes bigger as the preceding one (a numerical violation of the variational principle), we terminate the procedure and pick the smaller value as our final result. The difference between these last two values can be used as an estimate of the numerical inaccuracy. The errors will be further discussed below and in the next section when we compare our results

with related work (see Tables XV, XVI).

It should also be pointed out that the numerical analysis is conceptually very different from the computer algebraic treatment. As one cannot perform a Taylor expansion numerically, the expansion coefficients of M^2 have to be obtained by fitting polynomials to $M^2(m)$. Clearly, this is an additional source of errors, and one expects the results to be less accurate than those of the preceding sections. A cubic fit to the optimum values for $M^2 - 1$ in Table XI yields the following expansion coefficients of M^2 ,

$$M_1 = 3.62609 , \tag{4.1a}$$

$$M_2 = 3.33607 , \tag{4.1b}$$

$$M_3 = 0.22396 , \tag{4.1c}$$

which should be compared with the last line of Table V. To estimate the accuracy of these values we also show the results from a quartic fit,

$$M_1 = 3.62755 , \tag{4.2a}$$

$$M_2 = 3.31029 , \tag{4.2b}$$

$$M_3 = 0.32984 . \tag{4.2c}$$

Comparing (4.1) and (4.2) one finds that the stability of the fits is not too impressive in view of the accuracy we would like to achieve. In particular the third order coefficient is numerically difficult to determine. We estimate the relative accuracy as being 10^{-3} for M_1 , 10^{-2} for M_2 and 10^{-1} for M_3 . This is also confirmed by comparing with Table V.

For the Schwinger model it is possible to check the influence of higher particle sectors on the ‘pion’ mass squared by using the machinery developed in [38] for the wave functions of the higher Fock components. These are the amplitudes of finding not only two, but four, six, ... (anti-)fermions in the ‘pion’. In Table XII, we list the best values for $M^2 - 1$ including up to six-body wave functions. We also show the 2-, 4-, and 6-body content of the total wave function. It is known that the ‘pion’ is entirely 2-particle in the chiral limit [37]. For small mass, one therefore expects only small contributions from the higher Fock sectors. This is confirmed by the numerical results. Astonishingly, this feature persists up to values of at least $m = 0.5$ for the fermion mass. This fact is in agreement with the observation of Mo and Perry that the four-particle component of the wave function is less than 0.4 % for *all* values of the fermion mass [37]. A similar result has been found in the DLCQ calculations of [33]. In addition we note that there seems to be some interesting kind of hierarchy between the relative strengths of the contributions from different particle sectors. If we denote the $2k$ -particle amplitude in the wave function by f_{2k} , we find that $|f_2|^2 \gg |f_4|^2 \gg |f_6|^2$, the individual proportions being several orders of magnitude (see Table XII). Here, we explicitly see the magic of light-front field theory at work: high Fock components in bound states tend to be largely suppressed, at variance with the situation encountered in field theory quantized the standard way.

TABLE XII. Numerical Results for $M^2 - 1$ as a function of the fermion mass m , for $\alpha = 1$ (Schwinger model) including 2-, 4- and 6-body wave functions. The contributions of the different Fock sectors to the total wave function squared are given in percent.

| | $m = 0.0001$ | $m = 0.0005$ | $m = 0.001$ | $m = 0.005$ | $m = 0.01$ | $m = 0.05$ | $m = 0.1$ | $m = 0.5$ |
|-----------|--------------|--------------|-------------|-------------|------------|------------|-----------|-----------|
| $M^2 - 1$ | 0.000362793 | 0.00181481 | 0.00363055 | 0.0182179 | 0.0365968 | 0.189468 | 0.395400 | 2.66787 |
| % 2-body | 100.00 | 100.00 | 100.00 | 99.999990 | 99.999962 | 99.999213 | 99.997514 | 99.986816 |
| % 4-body | – | – | – | 0.000010 | 0.000038 | 0.000782 | 0.002474 | 0.013171 |
| % 6-body | – | – | – | – | – | 0.000005 | 0.000013 | 0.000013 |

From the point of view of the variational principle, the results shown in Table XII are a bit better (*i.e.* smaller) than those of Table XI (apart from the value for $m = 0.0005$), but the improvement is rather small. A cubic fit yields

$$M_1 = 3.62667 , \quad (4.3a)$$

$$M_2 = 3.23696 , \quad (4.3b)$$

$$M_3 = 0.36235 , \quad (4.3c)$$

and a quartic fit

$$M_1 = 3.62747 , \quad (4.4a)$$

$$M_2 = 3.20864 , \quad (4.4b)$$

$$M_3 = 0.60365 . \quad (4.4c)$$

Compared with (4.1) and (4.2) we do not find any absolute improvement in M_1 that could be distinguished from the numerical inaccuracy. For the coefficient M_2 , which in bosonization schemes is 3.3874, we even get the wrong tendency: it becomes smaller upon including higher Fock states. The inaccuracy for M_3 is so large that this coefficient is only determined in its order of magnitude.

Altogether, we arrive at the very important conclusion that the inclusion of higher particle sectors in the light-front bound state equation of the Schwinger model does not diminish the discrepancy between the results obtained via the 't Hooft-Bergknoff method and those from bosonization techniques.

Let us move to the 't Hooft model. If we put $\alpha = 0$ in the Schwinger model code above (Code I) we find the 'pion' mass squared for the 't Hooft model. The best values within the 2-particle sector are listed in Table XIII. Note that higher particle sectors are strictly suppressed in the large- N_C limit. Thus, there is no point in calculating these, unless one is interested in $1/N_C$ corrections to the 't Hooft model results [24] [34] [35].

In view of the restricted number of data points only a quadratic fit makes sense which yields

TABLE XIII. M^2 as a function of the fermion mass m , for $\alpha = 0$ ('t Hooft model), obtained with Code I

| m | 0.0001 | 0.001 | 0.01 | 0.1 |
|-------|-------------|------------|-----------|----------|
| M^2 | 0.000362795 | 0.00363109 | 0.0366342 | 0.398634 |

TABLE XIV. M^2 as a function of the fermion mass m , for $\alpha = 0$ ('t Hooft model), obtained with Code II

| m | 0.0001 | 0.001 | 0.01 | 0.1 |
|-------|-------------|------------|-----------|----------|
| M^2 | 0.000362795 | 0.00363118 | 0.0366341 | 0.398634 |

$$M_1 = 3.62754 , \tag{4.5a}$$

$$M_2 = 3.58796 , \tag{4.5b}$$

which is consistent with the results of Section III (see Table II). A second code (Code II), which was independently developed for the 't Hooft model [35] yields the results displayed in Table XIV. From a quadratic fit we obtain

$$M_1 = 3.62754 , \tag{4.6a}$$

$$M_2 = 3.58806 . \tag{4.6b}$$

Comparing with (4.5) we see that both codes yield the same results within the numerical accuracy. This is reassuring, since, as already stated, the codes were developed independently from each other.

A cubic fit to a total of 30 data points produced with Code II yields

$$M_1 = 3.62758 , \tag{4.7a}$$

$$M_2 = 3.58260 , \tag{4.7b}$$

$$M_3 = 0.06450 , \tag{4.7c}$$

in fair agreement with the variationally obtained values of Table II. To check the stability of this fit we can compare with the extension to fourth order,

$$M_1 = 3.62756 , \tag{4.8a}$$

$$M_2 = 3.58314 , \tag{4.8b}$$

$$M_3 = 0.06280 , \tag{4.8c}$$

$$M_4 = 0.001232 . \tag{4.8d}$$

This leads to an estimate of roughly 10^{-6} , 10^{-4} and 10^{-2} for the (absolute) numerical error in the first, second and third order coefficient, respectively. Furthermore it is gratifying to note that the fourth order coefficient, M_4 , is numerically small.

As is obvious from the discussion above, the numerical errors for the 't Hooft model are much smaller than those for the Schwinger model. The basic reason for this is the Schwinger model anomaly. Note that in the bound state equation the anomaly factor α multiplies an integral over the wave function. To evaluate this, one needs the wave function as a whole. In the 't Hooft model, on the other hand, this term is absent and the eigenvalues are dominated entirely by the endpoint behaviour of the wave function which is known exactly. This makes the numerical errors much smaller (see also Tables XV, XVI).

V. DISCUSSION AND CONCLUSION

In the preceding sections we have calculated the expansion coefficients M_i in the series

$$M^2 = \alpha + M_1 m + M_2 m^2 + M_3 m^3 \tag{5.1}$$

for the 'pion' mass squared of both the 't Hooft ($\alpha = 0$) and the Schwinger model ($\alpha = 1$). In order for the expansion (5.1) to make sense we have considered only small masses $m \ll 1$ *i.e.* $m \ll \mu_0$ in the original units. For the 't Hooft model we have $\mu_0^2 = g^2 N_C / 2\pi$ with $N_C \rightarrow \infty$, $g^2 N_C$ fixed. Thus, we are working in the *weak* coupling phase where the limit $N_C \rightarrow \infty$ ($g \rightarrow 0$), is taken *before* the limit $m \rightarrow 0$, or, equivalently, such that one always has $m \gg g \sim 1/\sqrt{N_C} \rightarrow 0$ [7] [42]. For the Schwinger model, $\mu_0^2 = e^2/\pi$, so that small fermion mass corresponds to *strong* coupling.

We have used analytical, computer algebraic and numerical methods of different accuracy. Nonetheless, the overall picture is intrinsically consistent. Our main findings are the following:

- (i) The first order coefficient, M_1 , in the expansion of the 'pion' mass squared is independent of the anomaly α , *i.e.* the same in both the 't Hooft and Schwinger model. This confirms the results of 't Hooft [2] [3] and Bergknoff [13].
- (ii) The 't Hooft-Bergknoff value, $M_1 = 2\pi/\sqrt{3}$, is a 'variational invariant': it does not get altered by extending the space of variational parameters. This has been checked analytically and numerically.
- (iii) In the Schwinger model, the 't Hooft-Bergknoff value does not change upon inclusion of higher particle sectors. Only the second and third order coefficients, M_2 and M_3 , are affected.
- (iv) Thus, for the Schwinger model, there remains a few percent discrepancy in the coefficients M_1 and M_2 compared to bosonization results.
- (v) The variational calculation yields the 'pion' wave function to a high accuracy. The endpoint behaviour is reproduced exactly (in leading order in m). The behaviour in the intermediate region, $0 < x < 1$, gets improved as can be seen from Fig. 3 below.

TABLE XV. The expansion coefficients M_i for the 't Hooft model ($\alpha = 0$). The errors of our results obtained within 2-particle Tamm-Dancoff (2PTD) approximation are estimated by comparing the last two lines in Table II (for the variational method) and the different polynomial fits (4.5 - 4.8) (for the numerical results). The numerical inaccuracies given in the last line were estimated by us using the polynomial fit method.

| | M_1 | M_2 | M_3 |
|------------------|-------------------------------|--------------------------------|--------------------------------|
| variational 2PTD | $2\pi/\sqrt{3} = 3.627599$ | $3.581055 \pm 3 \cdot 10^{-6}$ | $0.061793 \pm 3 \cdot 10^{-6}$ |
| numerical 2PTD | $3.62758 \pm 2 \cdot 10^{-5}$ | $3.5829 \pm 3 \cdot 10^{-4}$ | $0.064 \pm 1 \cdot 10^{-3}$ |
| 't Hooft [3] | $2\pi/\sqrt{3} = 3.627599$ | – | – |
| Burkardt [26] | $2\pi/\sqrt{3} = 3.627599$ | 3.5812 | – |
| Li [28] | 3.64 ± 0.06 | – | – |
| Li et al. [43] | 3.64 ± 0.03 | 3.60 ± 0.06 | 0.04 ± 0.04 |

In Table XV we summarize our optimum final results for the 't Hooft model ($\alpha = 0$) and compare with results that have been obtained previously.

Upon inspection of Table XV one finds a very good overall consistency of the results. All given values are in good agreement within error bars. The scale is set by the variational results which are the most accurate ones. They are matched by our numerical results as well as by previous analytical and numerical calculations.

As far as the latter are concerned, a few remarks are in order. The coefficients M_i displayed in the last line of Table XV are obtained by performing polynomial fits to the values calculated numerically in [43] (which basically agree with those from 't Hooft's original calculation displayed in Fig. 5 of [2]). The averaged result of the fits is shown including an estimate of the errors. It should also be stressed that the data in [43] are mainly obtained for $m > 0.5$ whereas the bulk of our values for the M_i are obtained for $m < 0.1$. Nevertheless, the agreement with our results is satisfactory within error bars.

From Table XV it is obvious that all numerical results favour the first order 't Hooft-Bergknoff value of $2\pi/\sqrt{3}$. This agreement is particularly gratifying for the data of [43] which were not obtained via LC techniques but within ordinary quantization and even within a different gauge, namely axial gauge. The agreement is therefore highly non-trivial [44].

For the Schwinger model, ($\alpha = 1$), we summarize our findings in Table XVI. For comparison we have also listed analytical results obtained via bosonization techniques and data which we extracted from polynomial fits to numerical LFTD [37], DLCQ [33] and lattice results [45]. The contents of Table XVI are graphically displayed in Fig. 2, where we have chosen rescaled units as in [22].

As already stated, due to the anomaly the numerical errors for the Schwinger model are at least an order of magnitude larger than for the 't Hooft model. In addition, the 2% discrepancy between our LC results and the analytic bosonization results does not get resolved. However, we have shown that the discrepancy is not due to (i) inaccuracies in the

FIG. 2. The rescaled ‘pion’ mass $\bar{M} = M/\sqrt{1+m^2}$ as a function of the fermion mass m . The short-dashed curve represents a ‘phenomenological’ parametrization for \bar{M} with $M^2 = 1 + M_1 m + 4m^2$, which becomes exact for very small and very large m and thus smoothly interpolates between the strong and weak coupling regions. The long-dashed curve is our second-order and the solid curve our third-order result. As expected, mass perturbation theory breaks down as m becomes of order 1. The crosses are the lattice results [45], the diamonds the lattice results [46], which go down to comparatively small masses, however with large errors. The circles are LFTD results [37], whereas the squares [33] and triangles [47], as quoted in [22], are DLCQ results. The values corresponding to the triangles are *not* included in Table XVI. The 2% discrepancy in M_1 is invisible within the resolution of the figure.

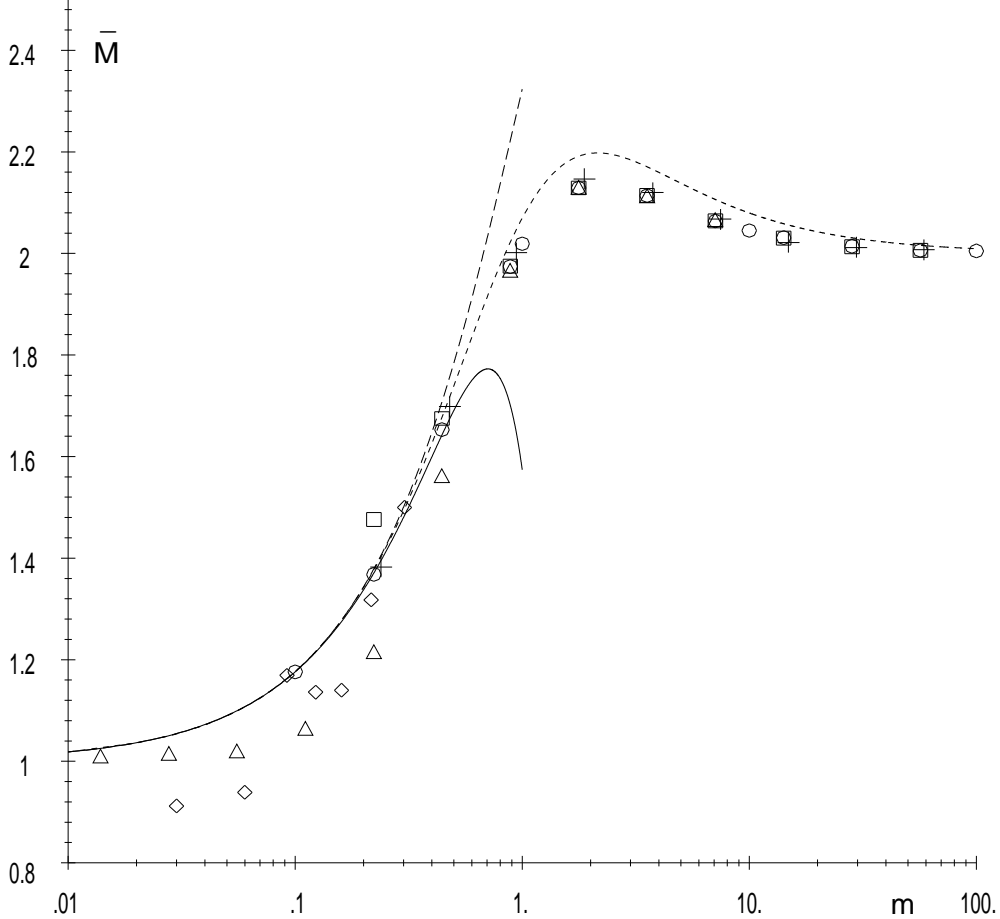


TABLE XVI. The expansion coefficients M_i for the Schwinger model ($\alpha = 1$). The errors for the variational 2-particle Tamm-Dancoff (2PTD) approximation are estimated by comparing the last two lines in Table V. The errors of our numerical calculations are obtained from comparing polynomial fits of different order to the numerical results of Tables XI and XII. Errors of other results are given where they could be estimated analogously.

| | M_1 | M_2 | M_3 |
|---------------------|------------------------------|--------------------------------|--------------------------------|
| variational 2PTD | $2\pi/\sqrt{3} = 3.627599$ | $3.308608 \pm 4 \cdot 10^{-6}$ | $0.348204 \pm 1 \cdot 10^{-6}$ |
| numerical 2PTD | $3.6268 \pm 8 \cdot 10^{-4}$ | 3.32 ± 0.02 | 0.28 ± 0.06 |
| numerical 6PTD | $3.6267 \pm 4 \cdot 10^{-4}$ | 3.22 ± 0.02 | 0.5 ± 0.1 |
| numerical 4PTD [37] | 3.62 ± 0.07 | 3.2 ± 0.3 | 0.3 ± 0.2 |
| DLCQ [33] | 3.7 ± 0.2 | 3.5 ± 0.3 | – |
| lattice [45] | 3.5 ± 0.2 | 3.7 | 0.02 |
| Adam [21] | $2e^\gamma = 3.562146$ | 3.3874 | – |
| Fields et al. [22] | $2e^\gamma = 3.562146$ | 3.387399 | – |

wave function or (ii) neglect of contributions from the next higher Fock sectors (four and six particles). It should be mentioned that other numerical methods (DLCQ, lattice) are by far too inaccurate to distinguish between the 't Hooft-Bergknoff and the bosonization value. We will come back to these issues in a moment.

As is well known, [22] [37] [48], the DLCQ data are comparatively inaccurate for small fermion mass m (*i.e.* large coupling). This is due to the fact that the dominating feature of the LC wave function, its endpoint behaviour, is not very accurately reproduced using an equally-spaced momentum grid. The poor convergence of DLCQ for small m has recently been overcome by incorporating the exact endpoint behaviour [48].

The lattice data generally suffer from the same disease of having rather large error bars for small m . The chiral limit, $m = 0$, can only be reached via extrapolation in a very inaccurate manner unless one uses the Schwinger result $M^2(m = 0) = 1$ as a bias [45]. A representative collection of lattice results for M_1 is given in Table XVII. For the convenience of the reader we also list the condensate $\langle 0|\bar{\psi}\psi|0\rangle = -M_1/4\pi$.

The values for the Schwinger model condensate in Table XVII should be compared with our results. If we assume that formulae (1.6) and (1.7) are directly applicable to our calculation we get

$$\langle 0|\bar{\psi}\psi|0\rangle = -\frac{M_1}{4\pi} = -\frac{1}{2\sqrt{3}} = -0.28868, \quad (5.2)$$

$$\langle 0|\bar{\psi}\psi|0\rangle = -\frac{1}{2\pi}\sqrt{\frac{M_2}{A+B}} = -0.28015, \quad (5.3)$$

while the standard result is

TABLE XVII. Lattice results for the first order coefficient M_1 and the (negative of the) condensate, $-\langle 0|\bar{\psi}\psi|0\rangle = M_1/4\pi$. The results are quoted in chronological order. They should be compared with the bosonization results, $M_1 = 3.562$, $-\langle 0|\bar{\psi}\psi|0\rangle = 0.283$ and the 't Hooft-Bergknoff values, $M_1 = 3.628$, $-\langle 0|\bar{\psi}\psi|0\rangle = 0.289$.

| | BKS76 ^a | CKS76 ^b | CH80 ^c | MPR81 ^d | HKC82 ^e | CK86 ^f |
|--------------------------------------|--------------------|--------------------|-------------------|--------------------|--------------------|-------------------|
| M_1 | 3.42 | 3.644 | 3.48 | 2.97 | 3.33 | 3.77 |
| $-\langle 0 \bar{\psi}\psi 0\rangle$ | 0.27 | 0.290 | 0.28 | 0.24 | 0.26 | 0.30 |

^aBanks, Kogut, Susskind [12]

^bCarroll, Kogut, Sinclair, Susskind [49]

^cCrewther, Hamer [45]

^dMarinari, Parisi, Rebbi [15]

^eHamer, Kogut, Crewther, Mazzolini [14]

^fCarson, Kenway [46]

$$\langle 0|\bar{\psi}\psi|0\rangle = -\frac{e^\gamma}{2\pi} = -0.28347. \quad (5.4)$$

As already mentioned in the introduction, the few percent discrepancies in M_1 and M_2 immediately affect the condensate. Note that the condensate value obtained from the second order coefficient is closer to the bosonization result, the relative error being 1.2 % compared to the 1.8 % at first order. Furthermore, the exact result (5.4) lies *between* our first and second order values, (5.2) and (5.3), so that their mean value, $\langle 0|\bar{\psi}\psi|0\rangle = -0.28442$, is much closer to (5.4), the error being only 0.3%. A similar reduction of errors is actually at work if one considers the 'pion' mass-squared of the Schwinger model as a function of m . The first order overshoots the bosonization value while the second order contribution is too small. Adding both one gets closer to the exact result, at least if the mass m is not too tiny. For the value of Fig. 1, $m = 0.1$, one finds to second order $M^2(0.1) = 1.39585$, while $M_{\text{Bos}}^2(0.1) = 1.39009$. The relative difference is only 0.4%. Possible resolutions of the discrepancies between (5.2), (5.3) and (5.4) will be discussed at the end of this section.

Apart from the 'pion' mass squared, the eigenvalue in the 't Hooft-Bergknoff equation, we have also calculated the associated eigenfunction, the light-cone wave function, with high accuracy. The latter has been obtained with high accuracy as can be seen from the good convergence of the alternatively defined mass squared coefficients, \tilde{M}_i towards the variational estimates, M_i (see Section III). If we denote $\phi_0(x) = x(1-x)$, our most accurate variational ansatz for the wave function can be written as

$$\phi[\beta, a, b, c, d] = \phi_0^\beta + a\phi_0^{\beta+1} + b\phi_0^{\beta+2} + c\phi_0^{\beta+3} + d\phi_0^{\beta+4}. \quad (5.5)$$

According to our mass perturbation theory, each of the variational parameters is expanded in powers of the fermion mass m , the coefficients being denoted $\beta_1, \beta_2, \beta_3, a_1, a_2$, etc. From 't Hooft's endpoint analysis, β is known exactly. It turns out to be independent of the anomaly (α) and thus is the same for the 't Hooft and Schwinger model. In Table XVIII we compare the exact expansion coefficients of β with their variational estimates. The best

TABLE XVIII. Comparison of the exact expansion coefficients of the endpoint exponent β with their best variational estimates for both the 't Hooft ($\alpha = 0$) and the Schwinger model ($\alpha = 1$).

| | β_1 | β_2 | β_3 |
|------------------------------|-----------------------------|-----------|-----------------------------|
| exact | $\sqrt{3}/\pi = 0.55132890$ | 0 | $-\beta_1/10 = -0.05513289$ |
| variational ($\alpha = 0$) | $\sqrt{3}/\pi = 0.55132890$ | 0.00051 | -0.053 |
| variational ($\alpha = 1$) | $\sqrt{3}/\pi = 0.55132890$ | 0.00063 | -0.053 |

TABLE XIX. Best estimates for the variational parameters in the LC wave function for both the 't Hooft ($\alpha = 0$) and Schwinger model ($\alpha = 1$).

| | a_1 | a_2 | b_1 | b_2 | c_1 | c_2 | d_1 | d_2 |
|--------------|-------|-------|-------|-------|-------|-------|-------|-------|
| $\alpha = 0$ | 0.92 | 1.19 | -2.2 | -3.0 | 7.0 | 9.2 | -9.9 | -11.8 |
| $\alpha = 1$ | 1.42 | 1.03 | -2.7 | -3.1 | 8.8 | 9.6 | -12.5 | -12.1 |

estimates for the other variational parameters are listed in Table XIX for both the 't Hooft and Schwinger model.

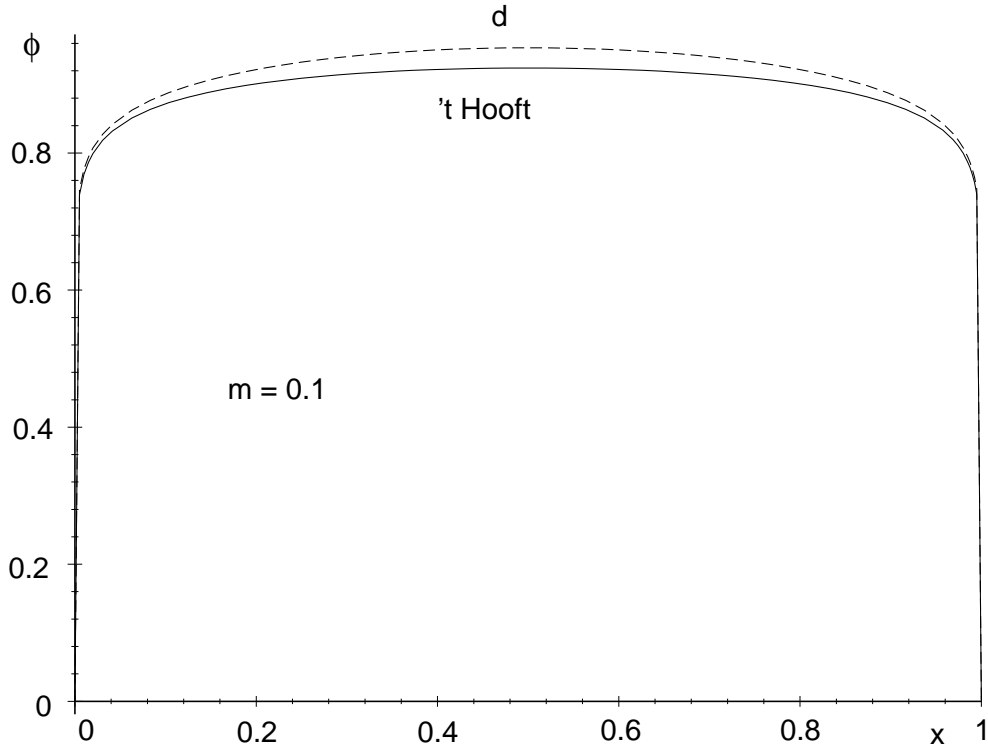
The errors in the coefficients are comparatively large and growing from the left to the right in Table XIX. Good numerical convergence is evident for the coefficients of a . For the other coefficients our method does not provide enough iteration steps to make convergence explicit. However, the sensitivity of the mass expansion coefficients M_i and the wave functions on the parameters b, c, d is very weak (see Fig. 3).

Let us finally investigate possible sources for the few-percent discrepancies in the Schwinger model results like for the condensate values, (5.2) and (5.3) *vs.* (5.4). First of all, it has to be reemphasized that the light-cone calculations are conceptually rather different from the usual treatment based on bosonization within standard equal-time quantization. We are studying the lowest lying meson as a relativistic fermion-anti-fermion bound state. The fermionic degrees of freedom are *explicitly* taken into account as they define our Fock basis. In the bosonized theory, which is a sine-Gordon model with the Lagrangian [8] [9]

$$\mathcal{L} = \frac{1}{2}\partial_\mu\phi\partial^\mu\phi - \frac{1}{2}\mu_0^2\phi^2 - cm\mu_0 \cos\sqrt{4\pi}\phi, \quad (5.6)$$

the 'pion' is the elementary particle described by the scalar field ϕ . One calculates its mass by perturbation theory in the 'coupling' $cm\mu_0$, $c = e^\gamma/2\pi$. In the bosonized theory, this 'coupling' is actually dependent on the normal-ordering scale used to renormalize the theory. The standard choice is the most natural one, namely the Schwinger boson mass μ_0 , which explicitly appears in the Lagrangian (5.6). It is, however, not very hard to determine the general scale dependence of quantities calculated within perturbation theory. All one needs is Coleman's re-normal-ordering prescription [50] which for the case at hand is

FIG. 3. The light-cone wave function of the 't Hooft model 'pion' for $m = 0.1$. The solid curve represents the result from 't Hooft's original ansatz, the dashed curve our best result (with maximum number of variational parameters). At the given resolution, however, the curves of *all* extensions of 't Hooft's ansatz (a, b, c, d) lie on top of each other.



$$N_{\mu_0} \cos \sqrt{4\pi} \phi = \frac{\mu}{\mu_0} N_{\mu} \cos \sqrt{4\pi} \phi . \quad (5.7)$$

Here, N_{μ_0} and N_{μ} denote normal-ordering with respect to μ_0 and μ , respectively. From (5.7) one derives the following identity for the boson mass squared (setting $\mu_0 = 1$),

$$\begin{aligned} M^2 &= 1 + M_1 m + M_2 m^2 + M_3 m^3 + \dots \\ &= 1 + M'_1 \mu m + M'_2 \mu^2 m^2 + M'_3 \mu^3 m^3 + \dots . \end{aligned} \quad (5.8)$$

In this expression, the M_i denote the coefficients calculated with the standard normal-ordering scale μ_0 , where all tadpoles can be set to zero, while the M'_i are calculated with normal-ordering scale μ , where one has non-vanishing tadpole contributions. In order that the 'pion' mass be scale independent one has to have that (upon reintroducing μ_0)

$$M'_n = \left(\frac{\mu_0}{\mu} \right)^n M_n . \quad (5.9)$$

We have checked this identity explicitly in the first two non-trivial orders of mass perturbation theory with the Lagrangian (5.6). It is also interesting to note that the scale

dependence of the coefficients might equivalently be associated with a multiplicative rescaling of the fermion mass m by defining $m' = \mu m$ and using m' as the expansion parameter in (5.8).

Now, the upshot of all this is the following. As we are working entirely in the fermionic representation, we do not a priori know, to which normal-ordering scale of the *bosonized* theory our results correspond. If we assume that it is not the Schwinger mass μ_0 but a different scale μ , we can match the first order coefficients by choosing

$$\mu = \frac{M_1}{M'_1} \mu_0 = \frac{e^\gamma}{\pi/\sqrt{3}} \mu_0 , \quad (5.10)$$

where M'_1 now denotes our light-front result. Quite a similar point of view has been taken by Burkardt in his paper on light-cone quantization of the sine-Gordon model [51]. However, as is obvious from (5.9), the change of scale (5.10) propagates systematically through all coefficients. In particular, if M'_1 is larger than the corresponding bosonization result, the same has to be true for all M'_i . Our coefficient M'_2 , however, already fails this requirement. We thus conclude that a possible scale dependence alone cannot explain the discrepancy.

An additional source of error could still be contributions from higher Fock sectors. We have shown numerically that the first few low orders have very little impact on the expansion coefficients M_i . The contribution from each Fock sector might thus be exponentially small. The whole series, however, if it could be summed up, might add something sizeable. Let us assume, for example, that the contribution of higher Fock sectors to M_2 has the following form²

$$\delta M_2 = \sum_{n=2}^{\infty} c_{2n}(m) , \quad (5.11)$$

where $2n$ is the label of the $2n$ -particle sector. If we had $c_{2n}(m) = e^{-2nm}$, summation of the series would yield $\delta M_2 = 1/2m + O(1)$ and thus effectively a contribution to the first order in m . As we are not able to calculate the real high order behaviour of the series in (5.11), we cannot, at the moment, make any definite conclusion about a possible relevance of such summation effects. All we can say is, that if such effects are present, they must be numerically small, *i.e.* at the few percent level.

As a first step towards getting some better control of higher particle sectors one would like to develop some tools to estimate their contributions analytically. This amounts to determine the coefficients $c_{2n}(m)$, at least for small n . So far, higher Fock states have only been included numerically.

It might also be interesting to calculate excited states. For the Schwinger model, this again requires the inclusion of higher Fock components as pointed out by Mo and Perry [37]. For the 't Hooft model, on the other hand, one can stay in the two-particle sector. One might then try to modify the variational procedure, basically by taking into account the growing number of nodes, with the aim to match the low energy spectrum with the high energy behaviour derived by 't Hooft. Work in these directions is underway.

²We thank M. Burkardt for suggesting the following example.

ACKNOWLEDGEMENTS

It is a pleasure to thank T. Sugihara for providing the numerical data yielding the fits (4.7) and (4.8). K.H. and T.H. would like to express their gratitude to the organizers of the 1997 Les Houches workshop on ‘Light-Cone Quantization and Non-Perturbative Dynamics’, in particular to P. Grangé, for providing such a stimulating atmosphere in which this work was finished. They thank the participants M. Burkardt and S. Pinsky for valuable discussions. T.H. is also indebted to C. Adam, F. Lenz, L. Lipatov, A. Neveu and B. van de Sande for useful hints and suggestions. T.H. and C.S. thank S. Simbürger for his assistance with some mathematical intricacies and E. Werner for continuous support and encouragement. K.H. acknowledges financial support provided by the Sumitomo foundation (No. 960517).

REFERENCES

- [1] J. Schwinger, Phys. Rev. **128**, 2425 (1962)
- [2] G. 't Hooft, Nucl. Phys. **B75**, 461 (1974)
- [3] G. 't Hooft, Lecture given at the International School of Subnuclear Physics, Erice, Italy, 1975; in: New Phenomena in Subnuclear Physics, Part A, A. Zichichi, ed., Plenum, New York, 1977
- [4] C. Adam, Ann. Phys. (N.Y.) **259**, 1 (1997)
- [5] E. Abdalla, M.C.B. Abdalla, Phys. Rep. **265**, 253 (1996)
- [6] E. Witten, Nucl. Phys. **B145**, 110 (1978)
- [7] A. Zhitnitsky, Sov. J. Nucl. Phys. **43**, 999 (1986)
- [8] S. Coleman, R. Jackiw, L. Susskind, Ann. Phys. (N.Y.) **93**, 267 (1975)
- [9] S. Coleman, Ann. Phys. (N.Y.) **101**, 239 (1976)
- [10] J. Lowenstein, J. Swieca, Ann. Phys. (N.Y.) **68**, 172 (1971)
- [11] J. Kogut, L. Susskind, Phys. Rev. D **11**, 3594 (1975)
- [12] T. Banks, J. Kogut, L. Susskind, Phys. Rev. D **13**, 1042 (1976)
- [13] H. Bergknoff, Nucl. Phys. **B122**, 215 (1977)
- [14] C.J. Hamer, J. Kogut, D.P. Crewther, M.M. Mazzolini, Nucl. Phys. **B208**, 413 (1982)
- [15] E. Marinari, G. Parisi, C. Rebbi, Nucl. Phys. **B190**, 734 (1981)
- [16] A. Smilga, Phys. Lett. **B278**, 371 (1992), and references therein
- [17] T. Heinzl, Phys. Lett. **B388**, 129 (1996)
- [18] M. Gell-Mann, R.J. Oakes, B. Renner, Phys. Rev. **175**, 2195 (1968)
- [19] E.V. Prokhvatilov, V.A. Franke, Sov. J. Nucl. Phys. **47**, 559 (1988); **49**, 688 (1989)
- [20] G. McCartor, Z. Phys. **C52**, 611 (1991); **C64**, 349 (1994); G. McCartor, D.G. Robertson, S.S. Pinsky, Phys. Rev. D **56**, 1035 (1997); A.C. Kalloniatis, D.G. Robertson, Phys. Lett. **B381**, 209 (1996); T. Heinzl, S. Krusche, E. Werner, Phys. Lett. **B256**, 55 (1991); **B275**, 410 (1992); J. Gamboa, I. Schmidt, L. Vergara, hep-th/9610173
- [21] C. Adam, Phys. Lett. **B382**, 383 (1996)
- [22] T.J. Fields, H.-J. Pirner, J. Vary, Phys. Rev. D **53**, 7231 (1996)
- [23] M.S. Marinov, A.M. Perelomov, M.V. Terent'ev, JETP Lett. **20**, 225 (1974)
- [24] K. Hornbostel, S.J. Brodsky, H.-C. Pauli, Phys. Rev. D **41**, 3814 (1990)
- [25] S. Coleman, Comm. Math. Phys. **31**, 259 (1973)
- [26] M. Burkardt, Ph.D. thesis, Erlangen, 1989, unpublished
- [27] F. Lenz, S. Levit, M. Thies, K. Yazaki, Ann. Phys. (N.Y.) **208**, 1 (1991)
- [28] M. Li, Phys. Rev. D **34**, 3888 (1986)
- [29] R.C. Brower, W.L. Spence, J.H. Weis, Phys. Rev. D **19**, 3024 (1979)
- [30] T. Maskawa, K. Yamawaki, Progr. Theor. Phys. **56**, 270 (1976)
- [31] H.-C. Pauli, S.J. Brodsky, Phys. Rev. D **32**, 1993, 2001 (1985)
- [32] A. Harindranath, R.J. Perry, K.G. Wilson, Phys. Rev. Lett. **65**, 2969 (1990)
- [33] T. Eller, H.-C. Pauli, S.J. Brodsky, Phys. Rev. D **35**, 1493 (1987); T. Eller, H.-C. Pauli, Z. Phys. **C42**, 59 (1989);
- [34] M. Burkardt, Nucl. Phys. **A504**, 762 (1989)
- [35] T. Sugihara, M. Matsuzaki, M. Yahiro, Phys. Rev. D **50**, 5274 (1994)
- [36] K. Aoki, T. Ichihara, Phys. Rev. D **52**, 6435 (1995)
- [37] Y. Mo, R.J. Perry, J. Comp. Phys. **108**, 159 (1993)

- [38] K. Harada, A. Okazaki, M. Taniguchi, Phys. Rev. D **52**, 2429 (1995)
- [39] I.M. Gelfand, G.E. Shilov, *Generalized Functions*, Academic, New York, 1964
- [40] W.A. Bardeen, R.B. Pearson, E. Rabinovici, Phys. Rev. D **21**, 1037 (1980)
- [41] K. Harada, T. Sugihara, M. Taniguchi, M. Yahiro, Phys. Rev. D **49**, 4226 (1994)
- [42] A. Zhitnitsky, Phys. Rev. D **53**, 5821 (1996)
- [43] M. Li, M. Birse, L. Wilets, J. Phys. **G13**, 915 (1987)
- [44] I. Bars, M.B. Green, Phys. Rev. D **17**, 537 (1978)
- [45] D.P. Crewther, C.J. Hamer, Nucl. Phys. **B170**, 352 (1980)
- [46] S.R. Carson, R.D. Kenway, Ann. Phys. (N.Y.) **166**, 364 (1986)
- [47] S. Elser, Ph.D. thesis, Heidelberg, 1994
- [48] B. van de Sande, Phys. Rev. D **54**, 6347 (1996)
- [49] A. Carroll, J. Kogut, D.K. Sinclair, L. Susskind, Phys. Rev. D **8**, 2270 (1976)
- [50] S. Coleman, Phys. Rev. D **11**, 2088 (1975)
- [51] M. Burkardt, Phys. Rev. D **47**, 4628 (1993)